Available online at www.sciencedirect.com
SCIENCE DIRECT®
Advances in Water Resources 26 (2003) 965–976
Advances in Water Resources
www.elsevier.com/locate/advwatres

A regression approach to estimating reactive solute uptake in advective and transient storage zones of stream ecosystems

Steven A. Thomas [a,*], H. Maurice Valett [a], Jackson R. Webster [a], Patrick J. Mulholland [b]

[a] Department of Biology, Virginia Tech, Blacksburg, VA 24061, USA
[b] Environmental Sciences Division, Oak Ridge National Laboratory, Oak Ridge, TN 37831, USA

Received 5 March 2002; received in revised form 24 March 2003; accepted 15 May 2003

Abstract

A method is developed, the Regression Partitioning Method (RPM), for estimating the proportion of reactive solute uptake occurring within transient storage zones of streams. The RPM is a technique for analyzing solute addition data in which whole stream uptake ($mg\,m^{-2}\,d^{-1}$) is determined from the longitudinal pattern in plateau tracer concentrations. At one location, a time series of samples are collected that define the 'rising limb' of the solute breakthrough curve. The *y*-intercept estimated by regressing a measure of reactive tracer availability (e.g. NO_3–^{15}N:Cl ratio) and the percentage of tracer that has resided within, and returned from, the transient storage zone (i.e. hyporheic zone) was used to predict channel-specific NO_3 uptake rates. Uptake within the transient storage zone of stream-derived material is calculated by difference. Several numerical steps are developed that link uptake rate estimates to first-order reaction rate constants (λ_C and λ_S, min^{-1}) more commonly used to describe solute behavior in one-dimensional transport models.

The RPM was used to analyze the results of 2 stable isotope additions performed in Snake Den Branch, a small headwater stream in western North Carolina, USA. Channel-specific uptake rates (U_C) ranged from 10.6 to 23.0 mg NO_3–N $m^{-2}\,d^{-1}$ and slightly exceeded uptake in the transient storage zone (U_S), which varied from 10.1 to 18.2 mg NO_3–N $m^{-2}\,d^{-1}$. Uptake within the transient storage zone accounted for 44–49% of the total uptake. λ_C and λ_S estimates ranged from 0.023 to 0.034 min^{-1} and 0.011 to 0.024 min^{-1}, respectively. These processing rates correspond to solute residence times of 30–44 min and 41–90 min in the channel and storage zones, respectively. Finally, we assess the sensitivity of our approach to variation in the subsurface uptake coefficient and differing proportions of uptake occurring within the hyporheic zone.
© 2003 Elsevier Ltd. All rights reserved.

1. Introduction

Channel morphology and catchment hydrology combine to establish a dynamic and diverse physical template in streams. An important attribute of this template is the exchange of water between advective and non-advective (transient storage) habitats [3]. In relatively small channels (i.e. where discharge (Q) < 1 $m^3\,s^{-1}$), hydrologic exchange with the transient storage zone can be rapid enough to completely entrain stream water within kilometers or even 100's of meters in the case of very small ($Q < 0.1$ $m^3\,s^{-1}$) streams [19,21,45]. When transient storage zones reflect hyporheic flow paths, greater hydrologic residence times are associated with increased contact between water and chemically and biologically active surfaces [6,14,49,50]. In such cases, biological processes often interact with hyporheic flow to create a gradient of oxidation–reduction states, supporting a suite of biogeochemical processes that rarely occur on the benthic surface of streams [1,9,12,24]. In addition, the location of the hyporheic zone at the groundwater–surface water ecotone provides this region a particularly strong influence over the form and abundance of dissolved constituents in both stream and ground waters. As a result, they may significantly influence the spatial and temporal heterogeneity of biotic processes in the stream benthos [11,21,23,34,38,48,51]. In all, a strong argument emerges for the ecological importance of the hyporheic zone and the need for an understanding of material movement through this zone.

The importance of the hyporheic zone is a function of residence time of hyporheic porewater [14,39,50], the

* Corresponding author. Present address: Eco-metrics, Inc., 322 SW 3rd St., Pendleton, OR 97801, USA.
E-mail address: sthomas@eco-metrics.com (S.A. Thomas).

0309-1708/$ - see front matter © 2003 Elsevier Ltd. All rights reserved.
doi:10.1016/S0309-1708(03)00083-6

physical extent of the hyporheic zone [21,53], and the rates at which specific processes occur within the interstitial environment [13,48]. A common technique for quantifying hyporheic residence time and extent is to conduct field releases of a conservative tracer and use an inverse modeling approach to estimate the specific temporal and spatial characteristics of the transient storage zone [5,10,45,50]. Though often equated, the transient storage and hyporheic zones are not equivalent. However, they must begin to overlap as the cross-sectional area of the storage zone (A_S) approaches the cross-sectional area of the channel (A). In streams with $A_S/A \geqslant 1$, one can reasonably assume that the transient storage zone is primarily hyporheic though the hyporheic environment may be more extensive than indicated by TS modeling. Under these conditions, transient storage modeling and related analyses may provide an effective means of assessing hyporheic characteristics.

In contrast, rates of biogeochemical processes within hyporheic sediments are most often determined using sediment incubation techniques of various forms [2,15,27,47]. Heterogeneity in local hydrologic conditions [31,54], hyporheic organic matter (OM) content [7,30,52], interstitial redox potential [1,9], and metabolic activity [13,27] makes it difficult to extrapolate rate information determined in sediment cores (cm) to the reach scale (10–100's of meters) at which these processes influence stream water chemistry under field conditions.

In recent years, transient storage modeling has been coupled with experimental introductions of nutrients such as ammonium–nitrogen (NH_4–N), nitrate–nitrogen (NO_3–N), and phosphate–phosphorus (PO_4–P) with the intent of elucidating the relationship between nutrient spiraling [37] and hyporheic zone characteristics [16,32,34,49,50]. In these experiments, nutrient uptake length is used as a measure of nutrient retention and is quantified at the reach scale by assessing the longitudinal decline in a reactive tracer (e.g., NO_3–^{15}N) after correcting for the influence of dilution. Fitting a negative exponential decay function (see Eq. (3)) to the field data predicts the first-order rate constant of longitudinal loss (m^{-1}), the inverse of which is equal to the uptake length (S_W, m). Combining S_W with nutrient concentration (C), stream depth (z) and velocity (u) leads to estimates of areal uptake rate (U, $mg\,m^{-2}\,d^{-1}$). Uptake rates calculated using the spiraling approach reflect the combined activity of the channel and transient storage zone, and no direct information is been gained regarding the relative importance of these environments. Rather, the importance of the transient storage zone has been inferred indirectly by conducting experiments across a gradient of conditions and statistically assessing the relationship between nutrient retention and the dimensions of the transient storage zone. This approach has led to conflicting results. Some recent studies suggest that nutrient retention is closely related to GW–SW exchange as evidenced by significant declines in uptake lengths for NO_3–N and PO_4–P with increasing A_S/A [8,29,32,34,50]. Others have argued that hyporheic influences are quantitatively insignificant [6,14], and a recent study showed little relationship between transient storage and nutrient retention [16]. A positive relationship between transient storage zone extent/residence time and nutrient retention depends on functional similarity in the transient storage zones of differing streams. However, transient storage zones and associated hyporheic environments are likely to be heterogeneous in time and space within and across streams and it seems unreasonable to suspect that biogeochemical processing will be consistent [26,49].

By and large, studies that partition channel and storage zone processing rates are rare, though some notable exceptions occur. Kimball et al. [28] and Runkel [40] estimated first-order rate constants for specific biogeochemical processes using field addition experiments and modeling to estimate activity within the advective channel and the transient storage zone. A short coming of these studies is that both the channel and storage zone rate constants were unknown and estimated simultaneously. An alternate approach was used by Mulholland et al. [34], who quantified the proportion of phosphorus uptake occurring within channel and transient storage regions of their study stream by examining the ratio of $^{33}PO_4$:Cl on the rising limb of a solute breakthrough curve. Estimates of surface uptake were calculated by determining the $^{33}PO_4$:Cl ratio one channel residence time (determined as reach length $(l) \div$ mean water velocity (u)) after the initiation of the experimental addition. The combined activity of surface and subsurface zones was determined from the $^{33}PO_4$:Cl ratio at plateau. The percentage of uptake occurring within the transient storage zone was estimated by difference.

Identifying the specific locations responsible for biological uptake of reactive solutes is of great interest to ecologists studying material processing in streams. Several recent studies have employed stable isotope approaches to elucidate the fate of nitrogen in streams [33,38,43], in part because stable isotope injections avoid the enrichment effects that compromise many solute injection experiments [17,36]. Though stable isotopes provide a powerful tool for the study of stream biogeochemistry, analysis of NO_3–^{15}N samples is labor intensive and expensive compared to traditional analytical methods. When such logistical constraints limit the number of samples that can be collected and analyzed, application of the 'rising limb' technique may be an attractive alternative for separating zones of reactive solute removal. The objective of this paper is to refine and extend the rising limb technique of Mulholland et al. [34], link this approach to the more frequently used one-dimensional reactive transport models, and examine the validity of our modified version of the rising limb approach.

2. Study site

Research was conducted in the Southern Appalachian Mountains at Coweeta Hydrologic Laboratory, Macon County, NC, USA. Tracer experiments were performed in Snake Den Branch, which drains watershed (WS) 19 (Fig. 1), a 28 ha (70 acre) catchment that ranges in elevation from 796 m (2611 ft) at a V-notch weir established near the confluence of Snake Den Branch and Ball Creek to 1119 m (3671 ft) at the top of the watershed. The climate is typical of the southern Appalachian area. Mean annual temperature is 13 °C and the growing season extends from April to October. Average annual rainfall is approximately 200 cm distributed evenly among months with less than 2% of annual precipitation falling as snow. Vegetation in WS 19 is dominated by large oak-hickory stands with cove hardwoods common along the stream channel. An extensive understory of mountain laurel (*Kalmia latifolia* L.) and rhododendron (*Rhododendron maximum* L.) is typical in this area and provides a year-round canopy over Coweeta streams, which decreases light to very low levels (i.e. 2–5% of incident). Between December 1948 and March 1949, all laurel and rhododendron growing in WS 19 were cut with hand tools as part of an experimental assessment of water yield [25], but no manipulation of WS 19 has occurred since that time.

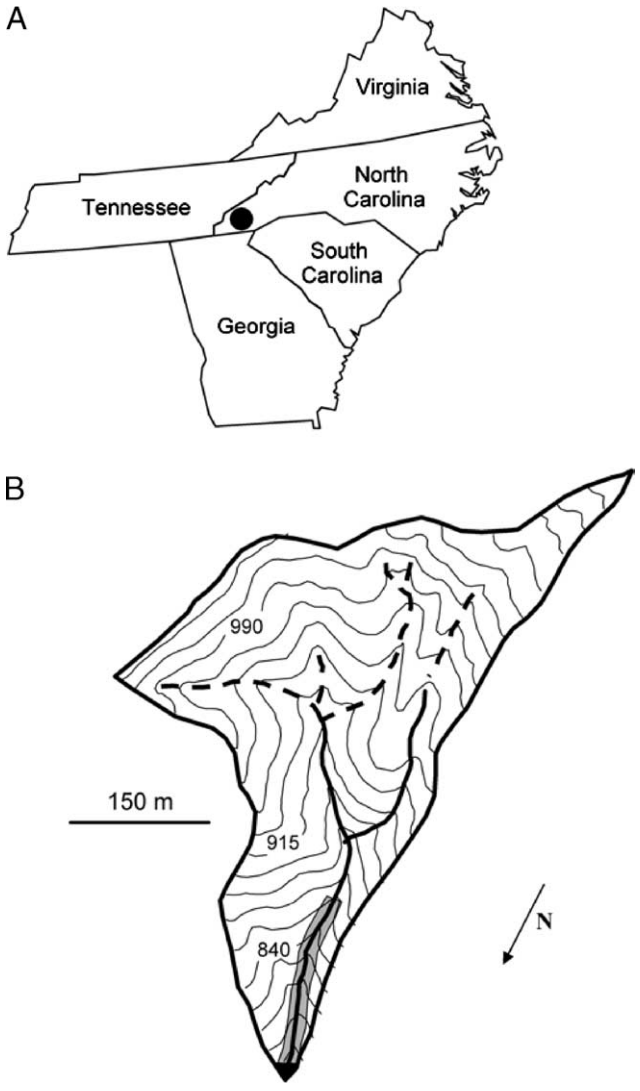

Fig. 1. (A) Location of the Coweeta Hydrologic Laboratory, Macon Co., NC, USA. (B) Map of watershed 19 and Snake Den Branch. Contour lines are in 20 ft intervals. Thick lines are watershed boundaries or perennial portions of the stream. Dashed lines are channels with intermittent flow. Solute injection experiments were conducted over 200 m of stream length located up gradient from the weir.

Parent lithology in the area is crystalline rocks of pre-Cambrian age composed of various granite mica schists and gneisses, primarily the Carolina gneiss [22]. Long (i.e. 50–100 m) reaches of exposed bedrock are evident along Snake Den Branch were stream gradient can be steep (≈30–40%) and these alternate with segments filled with poorly sorted colluvial material that serves as a good conduit for percolation of near-stream ground water. Solute injection experiments were carried out over the downstream 200 m (Fig. 1) of Snake Den Branch where the stream channel is composed of an upstream segment (≈50 m long) of exposed bedrock, a 100-m segment of poorly sorted colluvial sediments, and a downstream bedrock reach of approximately 50 m length. Bedrock reaches were generally free of smaller sediments, debris dams, and coarse particulate organic matter (CPOM), but a semi-aquatic moss heavily colonized lateral portions of the channel. Colluvial reaches retained larger amounts of OM, a diverse range of sediment particle sizes, and tracer concentrations measured in monitoring wells established within the colluvial plugs indicated evident interaction between surface and interstitial water.

3. Methods

3.1. Solute injection experiments

Co-injections of conservative (NaCl) and non-conservative ($K^{15}NO_3$) solutes were performed in Snake Den Branch on two occasions during 1999–2000. Injections of approximately 12-h duration were executed in late summer (September 1999) and spring (May 2000). Solute injections were designed to increase Cl concentrations 10–15 mg L^{-1} above background (with an associated increase in electrical conductivity of approximately 40–60 S cm^{-1}) and elevate ^{15}N of the NO_3–N pool to 40,000‰. Injectate solutions were introduced to surface water at a steady rate by a metering pump (Fluid Metering Inc., New York), which was calibrated frequently during injections. During all injections, tracers were added to the stream at a point of natural

constriction followed by a 10-m reach of turbulent flow to ensure adequate mixing. Downstream sampling locations were established 30–150 m below the injection site. Background samples for Cl, NO_3–N, and NO_3–^{15}N were collected from surface water at all sampling locations prior to injection. Following correction for background concentrations, Cl concentrations collected under fully mixed conditions were used to determine discharge.

Monitoring electrical conductivity at a downstream transect 100–150 m below the injection site generated solute breakthrough curves. Automated sondes (Hydrolab Model 4A) placed in mid-stream at the downstream monitoring station recorded electrical conductivity (± 0.1 S cm^{-1}) at 1-min intervals from 30 min before initiation of the injection until conductivity returned to background values. Following completion of each injection, conductivity values were downloaded from the sonde and converted to Cl concentrations using standard curves. These data were then used for one-dimensional modeling of solute transport.

3.2. Rising limb sampling

To guide surface water sampling of the rising limb, electrical conductivity was monitored with a YSI Model 55 Conductivity Meter (YSI Inc, Yellow Springs, Ohio, USA). A total of 10 samples were taken during the course of the arrival of the solute plume with sampling frequency initially high then more infrequent as tracer concentration approached steady state. Acid-washed 4-L Nalgene® polypropylene bottles were used for sample collection. Samples were collected from 2 in. PVC pipes secured in the streambed to create free-flowing spouts for rapid collection of stream water. Bottles were thoroughly rinsed with water from the spout before collecting 3–4 L samples for solute analysis. Once tracer had reached steady state throughout the study reach (as indicated by stable conductivity values at the downstream sampling location), replicate ($n = 3$–5 samples per location) samples were collected at each transect in the manner described above. All samples were filtered in the field using a Geotech® peristaltic pump (Geotech Inc., Denver, CO) equipped with a 20 cm in-line filter housing a 14.2 cm Whatman® GFF filter (pore size = 0.7 μm). Care was taken to avoid cross-contamination of samples by filtering samples in increasing order of tracer content and by thorough rinsing (deionized water followed by sample) of the filtration apparatus between samples. Samples were immediately placed on ice and returned to the laboratory at Virginia Tech within 24 h.

3.3. Laboratory sample processing

In the laboratory, 50-ml aliquots of the samples were removed and used immediately for analysis of Cl and NO_3–N using a Dionex® 500 Ion Chromatograph equipped with an AS14 anion detection column. The remainder of the sample was used to analyze NO_3–^{15}N content following the methods described by Sigman et al. [42]. Briefly, 1-L samples of water were spiked with NO_3–N to adjust ^{15}N to levels acceptable for most mass spectrometry laboratories (≈4000‰), and boiled under basic conditions to concentrate NO_3–N and drive off NH_3. Then $^{15}NO_3$ was converted to ammonia by addition of Devarda's Alloy, diffused into the bottle headspace under basic conditions and sorbed on an acidified glass fiber filter, sealed within a teflon filter pack floating on the liquid surface. The sorption process was allowed to proceed for 7 days, after which time filters were collected and analyzed using a Finnegan MAT.

3.4. Advection, dispersion and transient storage

Variables describing the interaction between the free-flowing stream channel and transient storage zones were estimated using a combination of field experiments and an advection–dispersion with storage model (ADSm) [4,18,41].

$$\frac{\partial C}{\partial t} = -\frac{Q}{A}\frac{\partial C}{\partial x} + \frac{1}{A}\frac{\partial}{\partial x}\left(AD\frac{\partial C}{\partial x}\right) + \frac{q_L^{in}}{A}(C_L - C) + \alpha(C_S - C) - \lambda_C(C) \quad (1)$$

$$\frac{\partial C_S}{\partial t} = \alpha\frac{A}{A_S}(C - C_S) - \lambda_S C_S \quad (2)$$

where C, C_L, and C_S equal the solute concentration (M L^{-3}) in the channel, in lateral inflow, and in the storage zone, respectively. Similarly, Q represents stream discharge (L^3 T^{-1}) and q_L^{in} equals lateral inflow (L^3 T^{-1}). A and A_S are the mean cross-sectional area (L^2) of the channel and the transient storage zone, respectively. D is the coefficient of dispersion (L^2 T^{-1}). α is the transient storage zone exchange rate (T^{-1}). λ_C and λ_S are first-order decay coefficients for the channel and the storage zone, respectively. Finally, t is time (T) and x is distance (L). M, L, and T represent mass, length, and time, respectively.

In estimating transient storage characteristics, the ADSm was fit to specific conductance data, recorded at 5 min intervals (using a Hydrolab™ minisonde). Parameter estimation relied on an automated least square method (Hart 1995) and on visual inspection. Best fit versions of the ADSm produced estimates of mean water velocity ($u = Q/A$), α, and A_S. Because Cl^-, and therefore specific conductance, was assumed to behave conservatively, the first-order decay coefficients (λ_C and λ_S) were set to zero for the transient storage modeling. Several metrics useful in assessing transient storage zone characteristics were also computed. Those metrics include the mean residence time in the storage zone (T_S)

[44], the exchange length of water (L_S) [35], and the storage zone exchange flux (q_s) [21]. In addition, the median residence time of water within the study reach (T_{med}), the fraction of T_{med} attributable to transient storage (F_{med}) and a length standardized version of F_{med} (F_{med200}) were derived following the methods of Runkel [39].

3.5. Determining percent of uptake occurring in the transient storage zone: the Regression Partitioning Method (RPM)

Our refinement of the Mulholland et al. [34] approach combines the empirical workings of nutrient spiraling and transient storage models. First, we estimate nutrient uptake lengths (S_W; the average distance traveled by a reactive solute) using methods common in studies of nutrient spiraling and retention. Briefly, solute releases continued until plateau conditions were established (indicated by steady-state specific conductance readings), at which time replicate samples of chloride and NO_3–^{15}N were collected from 4–5 locations longitudinally distributed downstream of the solute release point. S_W estimates were computed by linearly regressing the natural log transformed plateau NO_3–^{15}N:Cl ratios (R_X) against longitudinal distance (x):

$$\ln R_X = \ln R_0 - kx \tag{3}$$

where R_0 is the NO_3–^{15}N:Cl ratio at 0 m and k is the longitudinal loss rate (m^{-1}). S_W is equal to the inverse of k. Whole stream estimates of NO_3–N uptake (U, mg NO_3–N $m^{-2}\,min^{-1}$) are calculated using:

$$U = \frac{QC}{wS_W} \tag{4}$$

where w is mean stream width (m) [37].

In estimating the percentage of U occurring in the channel and transient storage zones, our basic premise is that the ratio of the reactive to conservative solute (R; which equals NO_3–^{15}N:Cl in this study) should decline as the percentage of added solute that has exchanged with the transient storage zone increases. Early in a solute breakthrough curve, R will reflect assimilatory activity occurring in the water column. As the breakthrough curve proceeds, R is increasingly influenced by activity associated with the benthic surface. As the breakthrough curve of tracer solute proceeds towards plateau, an increasing percentage of the arriving tracers have resided in, and returned from, the transient storage zone and R progressively reflects the activity occurring within that environment.

The percentage of conservative tracer that has cycled through the storage zone ($TS_{\%}$) was determined by estimating the temporal pattern that would have occurred had none of the conservative tracer returned from storage (i.e. the channel comprised only of water that has never entered the storage zone) [18]. This assumption effectively sets $(\alpha A)/A_S = 0$, reducing Eqs. (1) and (2) to:

$$\frac{\partial C_M}{\partial t} = -\frac{Q}{A}\frac{\partial C_M}{\partial x} + \frac{1}{A}\frac{\partial}{\partial x}\left(AD\frac{\partial C}{\partial x}\right) + \frac{q_L^{in}}{A}(C_L - C_M) + \alpha C_M \tag{5}$$

where C_M is the modified chloride concentration resulting from one-way exchange with the storage zone. The $TS_{\%}$ for each time step was calculated from the conservative solute concentrations predicted by the modified (C_M) and original (C) transient storage model outputs:

$$TS_{\%} = \frac{C - C_M}{C} \times 100 \tag{6}$$

To calculate the value of NO_3–^{15}N:Cl at $TS_{\%} = 0$ (R_C; activity of the advective compartment), NO_3–^{15}N:Cl ratio (R) data collected after the influence of advection and dispersion (Fig. 2) where regressed against $TS_{\%}$:

$$R = R_C + (\beta \times TS_{\%}) \tag{7}$$

where R_C represents the NO_3–^{15}N:Cl ratio at the downstream station that would have occurred in the absence of a transient storage zone. The longitudinal loss rate solely due to activity in the advective zone (k_C) was calculated by substituting R_C into Eq. (3) and solving for k. The inverse of k_C is equal to the channel-specific uptake length, S_C. Uptake within the advective channel (U_C) was calculated by substituting S_C for S_W in Eq. (4). Uptake in the transient storage zone (U_S) was determined by difference ($U_S = U - U_C$). Storage zone-specific longitudinal loss rate (k_S) was calculated similarly ($k_S = k - k_C$) and storage zone-specific uptake lengths (S_S; uptake length in the channel that would have occurred had $k_C = 0$) were calculated as the inverse of k_S. The first-order decay constant for NO_3–^{15}N in the channel (λ_C; min^{-1}) was calculated as:

$$\lambda_C = k_C\frac{Q}{A} \tag{8}$$

Similarly, the decay rate for the storage zone (λ_S) was determined using:

$$\lambda_S = k_S\frac{Q}{A_S} \tag{9}$$

In order to assess the confidence in our estimate of λ_S, we conducted model runs with λ_S values ranging from 0.01× to 100× the predicted value while holding all other variables constant.

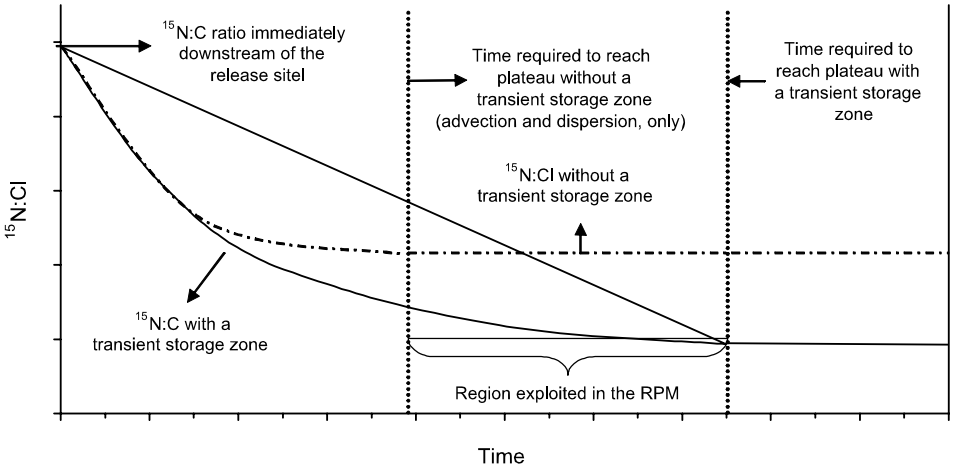

Fig. 2. A theoretical example of the change in NO_3–^{15}N:Cl ratio (R) through time at a location some distance downstream of an experimental solute addition point. The dashed and solid lines illustrate the expected temporal pattern in R in the absence and presence of a transient storage zone, respectively.

4. Results

4.1. Hydrology and transient storage

Flow conditions in Snake Den Branch were consistent between experiments (Table 1). Discharge was less than 5 $L\,s^{-1}$ across each experiment, but increased slightly from 2.63 $L\,s^{-1}$ in September 1999 to 4.79 $L\,s^{-1}$ in May 2000. Lateral inflow ranged from 0.005 to 0.010 $L\,s^{-1}\,m^{-1}$ resulting in a 19% and 22% increase in discharge over 152 and 107 m reach lengths in September and May, respectively. Mean water velocity (u) in September was 0.05 $m\,s^{-1}$ and increased slightly to 0.08 $m\,s^{-1}$ in May (Table 1). Mean water depth remained effectively constant (≈0.06 m), varying by less than 0.005 m between dates. Channel width in September and May was 1.12 and 1.13 m, respectively (Table 1).

Table 1
Hydrological characterization of Snake Den Branch, North Carolina

Variable	Units	September 1999	May 2000
Reach length	m	152	107
Discharge (Q; at 0 m)	$L\,s^{-1}$	2.63	4.79
Width	m	1.13	1.12
Velocity (u)	$m\,s^{-1}$	0.050	0.083
T_{med}	min	75.0	32.4
A	m^2	0.068	0.067
α	min^{-1}	0.0180	0.0252
A_S	m^2	0.110	0.090
A_S/A		1.62	1.33
T_S	min	90	53
L_S	m	168	198
HRF	$min\,m^{-1}$	0.54	0.27
q_s	$m^2\,min^{-1}$	0.00122	0.00169
F_{med}		0.28	0.19
F_{med200}		0.33	0.38

See text for variable descriptions.

Despite the abundance of bedrock outcroppings characteristic of the study reach, solute transport modeling revealed substantial transient storage, which was relatively consistent through time. For example, the absolute size of the transient storage zone (A_S) and it relative extent (A_S/A) varied from 0.9 to 1.1 and 1.3 to 1.7 m^2, respectively. The coefficient of exchange between the advective zone and the storage zone (α) was relatively high and ranged from 0.0180 to 0.0252 min^{-1}. The mean residence time in the transient storage zone (T_S) varied from a low of 53 min in May to 90 min in September. Hydrologic turnover lengths (L_S) varied from 168 to 198 m with maximum L_S occurring in March. The storage zone exchange flux (q_s) ranged from 0.00122 to 0.00169 $m^2\,min^{-1}$. Recently, Runkel [39] developed a unique transient storage metric that incorporates information on advective velocity, storage zone extent, and storage zone exchange rates. The resulting metric, F_{med}, reflects the fraction of the median travel time attributable to the transient storage. In this study, F_{med} equaled 0.19 and 0.28 in May and September, respectively. Because F_{med} is reach length sensitive, a reach length standardized version of the metric based on a 200 m reach length (F_{med200}) also was calculated and equaled 0.33 in September and 0.38 in May.

4.2. Whole stream NO_3–N dynamics

Background NO_3–N concentrations varied among seasons in Snake Den Branch. Concentrations in September averaged 11.7 ± 1.5 $\mu g\,L^{-1}$. By winter (March) concentrations had decreased nearly fourfold to 3.2 ± 0.1 $\mu g\,L^{-1}$, and they remained low in May (3.7 ± 0.1 $\mu g\,L^{-1}$). Among injections, longitudinal loss rate coefficients (k) varied little, ranging from 0.0133 to 0.0136 m^{-1}. Likewise, estimates of NO_3–N uptake

Table 2
Nitrate–N retention and uptake parameters for Snake Den Branch, North Carolina

Compartment	Variable	Units	September 1999	May 2000
Whole stream	NO_3–N	$mg\,L^{-1}$	11.7 ± 1.5 (29)	3.7 ± 0.1 (29)
	k	m^{-1}	0.0136	0.0133
	S_W	m	73	75.0
	U	$mg\,m^{-2}\,d^{-1}$	41.2	20.8
Advective channel	k_c	m^{-1}	0.0076	0.0068
	S_C	m	132	146
	U_C	$mg\,m^{-2}\,d^{-1}$	23.0	10.6
	λ_C	min^{-1}	0.023	0.034
	T_{NC}	min	43.7	29.4
Transient storage	k_s	m^{-1}	0.0060	0.0065
	S_S	m	166	154
	U_S	$mg\,m^{-2}\,d^{-1}$	18.2	10.1
	λ_S	min^{-1}	0.0112	0.024
	T_{NS}	min	89.3	41
U_S/U			0.44	0.49
Reaction significance factor (RSF)			0.92	0.70

Nitrate–N values are SE (n) for each sampling date. TSZ is the transient storage zone. See text for all other symbols.

length (S_W) were conservative between experiments, equaling 73 and 75 m for September and May, respectively (Table 2). N uptake rates varied among dates, largely due to variation in NO_3–N availability (i.e. fourfold range in concentration). Estimates of whole stream NO_3 uptake rates (U) were greater in September than in May (41.2 and 20.8 mg NO_3–N $m^{-2}\,day^{-1}$, respectively).

4.3. Determining uptake in the transient storage zone using the regression partitioning method

We first calculated the percentage of tracer that has resided in the storage environment ($TS_{\%}$) for each point in time that a sample was collected. Because samples were only collected from the rising limb and plateau of the solute breakthrough curves, maximum $TS_{\%}$ was constrained by the plateau condition (steady-state tracer concentrations throughout the study reach). Maximum $TS_{\%}$ in September, March, and May were 62.2% and 43.6%, respectively.

In applying the RPM, a distinct break in the curve relating R and $TS_{\%}$ was evident for each experiment and consistently corresponded to the $TS_{\%}$ occurring one reach residence time (T_R; calculated as reach length divided by average surface water velocity) [34] after the initiation of the experiment. Water samples collected prior to T_R represent parcels traveling the reach at the upper end of the velocity distribution. Presumably tracer within these samples have had less interaction with the stream bed surface than water parcels traveling at, or near, the mean velocity. In each application, it is interesting to note that R appeared to converge on the value expected at the tracer release point (0 m; Fig. 3). This observation suggests that little or no uptake of NO_3–N occurred in the water column.

Because our intention was to discriminate between uptake occurring in the channel from that occurring in the transient storage zone, we began the RPM analysis after the time at which plateau would have occurred had advection and dispersion alone controlled the solute breakthrough curve (Fig. 2). This time was calculated by running the best fit ADSm with α set to 0. For samples collected after this time, a significant ($p < 0.05$) regression was observed between R and $TS_{\%}$ in each month (Fig. 3). Regression results (e.g. R_0) were used to calculate channel-specific longitudinal loss coefficients (k_C), channel-specific uptake lengths (S_C), and channel-specific uptake rates (U_C). Like S_W, S_C estimates were similar between months varying by less than 10%. In contrast, U_C estimates were considerably greater in September than in May. Temporal rate constants for NO_3–N uptake in the channel (λ_C) increased with each injection from 0.023 min^{-1} in September to 0.034 min^{-1} in May (Table 2). These λ_C estimates translate to assimilatory residence times ($T_{NC} = 1/\lambda_C$) of 44 and 29 min, respectively.

Storage zone-specific uptake lengths (S_S) were longer, but similar, to S_C estimates (Table 2). Area-specific uptake rates in the storage zone (U_S) were 10.1–18.2 mg N $m^{-2}\,day^{-1}$ and accounted for 49% and 44% of whole stream uptake in May and September, respectively. Temporal loss rate constants for the transient storage zone (λ_S) were less than those calculated for the channel, resulting in longer assimilatory residence times in the storage zone (T_{NS}; Table 2).

Harvey and Fuller [20] proposed a dimensionless significance factor for chemical reactions in the hyporheic zone (RSF) in which

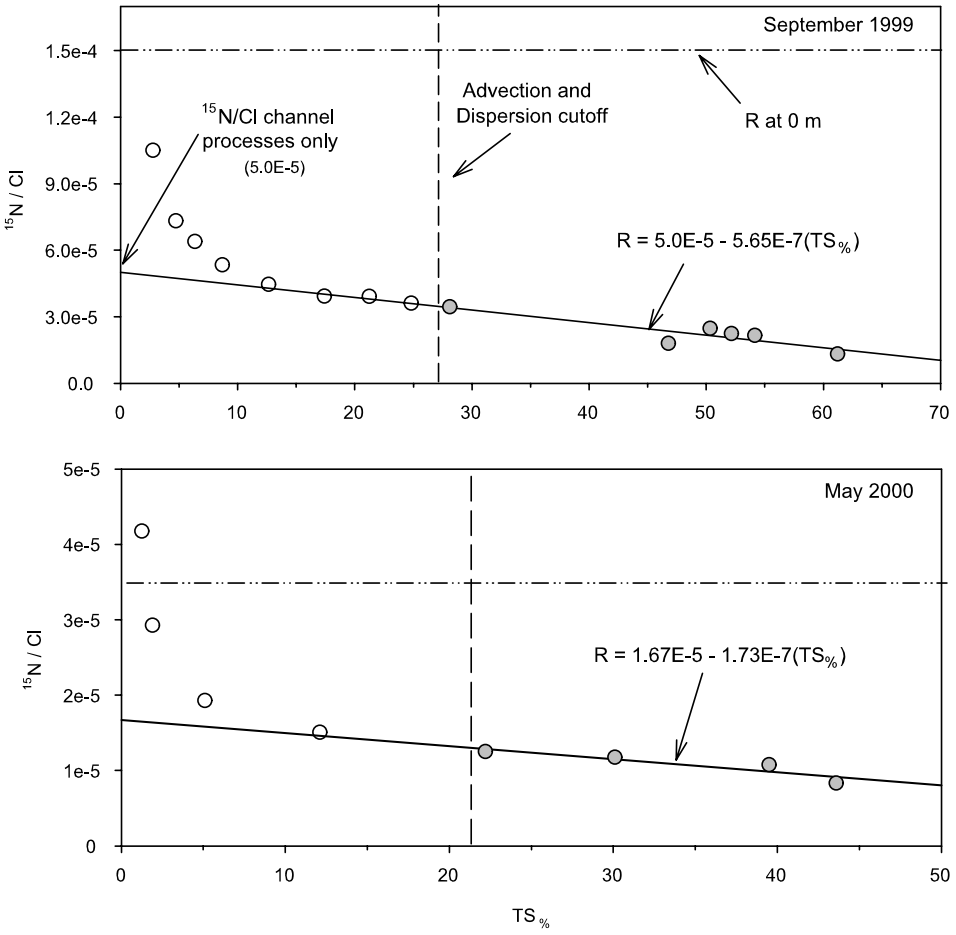

Fig. 3. Regressions between the ratio of reactive to conservative solute (NO_3–^{15}N:Cl) and the percentage of water that has resided within the transient storage zone ($TS_{\%}$). All regressions were significant ($p < 0.05$).

$$\mathrm{RSF} = \frac{\lambda_S T_S L}{L_S} \tag{10}$$

where L is stream reach length. They suggested that RSF values greater than 0.2 characterize reaches where chemical reactions in the hyporheic zone are fast enough to exert a cumulative influence on downstream water chemistry. In this study, RSF equaled 0.92 and 0.70 in September and May, respectively (Table 2).

4.4. Assessing the performance of the RPM in estimating λ_S

Incorporating λ_C and λ_S values into the one-dimensional reactive solute model (Eqs. (1) and (2)) and applying the values estimated by the RPM generated a temporal pattern of normalized concentrations of Cl and NO_3–^{15}N (C/C_0) that closely matched field measurements from each experiment (Fig. 4). As a means of assessing the sensitivity of the one-dimensional reactive solute model to variation in λ_S and at the same time address the ability of the RPM to estimate λ_S, we systematically altered λ_S from our May experiment while holding all other parameters constant. The resulting curves (Fig. 5) suggest that while the earliest points may be adequately represented by lower values of λ_S, later values may be over estimated. Altering λ_S by orders of magnitude resulted in significant deviations from the observed data. Thus, it appears that the RPM provides a reasonable estimate of λ_S given relatively few data.

5. Discussion

Previous studies of nutrient dynamics and GW–SW exchange have been combined to generate a conceptual model of solute retention in streams that emphasizes both characteristics of GW–SW interaction and rates of biological and chemical processes [46,50]. Specifically, ecosystem retention is portrayed as the product of water residence time (i.e. hydrologic retention) and the sum of biological and chemical processes that sequester or transform nutrients [13,50]. Greater GW–SW interaction increases hydrologic retention, enhancing nutrient processing through increased contact between solutes

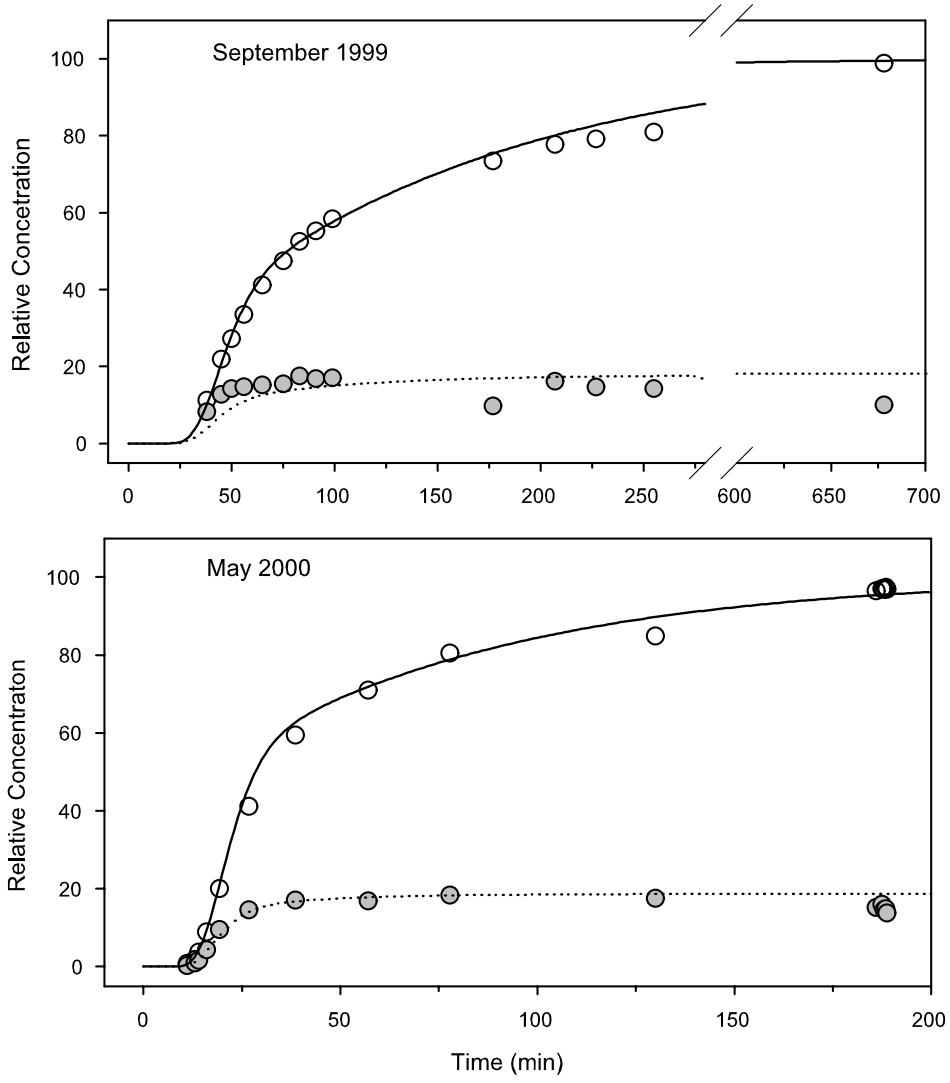

Fig. 4. The relationship between the field data and predicted values using a one-dimensional transport model with transient storage and reactive uptake. The uptake coefficients are first-order rate constants (λ and λ_S) derived from the Regression Partitioning Method.

and biologically and chemically active mineral surfaces [19]. The impetus for developing the regression partitioning method is provide a technique for directly quantifying the role of hyporheic/transient storage zones in stream biogeochemistry.

Development of the RPM was initiated as a means of refining the analysis of Mulholland et al. [34]. The method relies on a linear decline in the ratio of reactive to conservative tracer as the amount of conservative tracer experiencing residence in the storage environment increases. Initially, data collected after one reach residence time ($T_R = L/u$) were used in the analysis. However, simulations indicated that dispersion alone causes R to continue to decline after that time (Fig. 2). Therefore, the RPM exploits those data collected after the influence of dispersion and may be difficult to employ in streams in which the influence of transient storage on the solute breakthrough curve is minor in comparison to that of dispersion.

In Snake Den Branch, which has a relatively large transient storage zone, the RPM proved effective in partitioning retention between the advective (channel) and transient storage zones. In part, this conclusion is based on the observation that estimates of λ_C and λ_S predicted NO_3–^{15}N fluxes that matched the observed data in magnitude and pattern. The sensitivity analysis (Fig. 5) demonstrated that the form of the reactive solute breakthrough curve changed considerably as λ_S varied. Low values of λ_S generate a breakthrough profile that closely resembles the conservative tracer in shape (Fig. 4). Large values of λ_S produce a pattern resembling that produced by an advection and dispersion model lacking transient storage. Large λ_S render the storage zone an efficient sink from which reactive solutes fail to

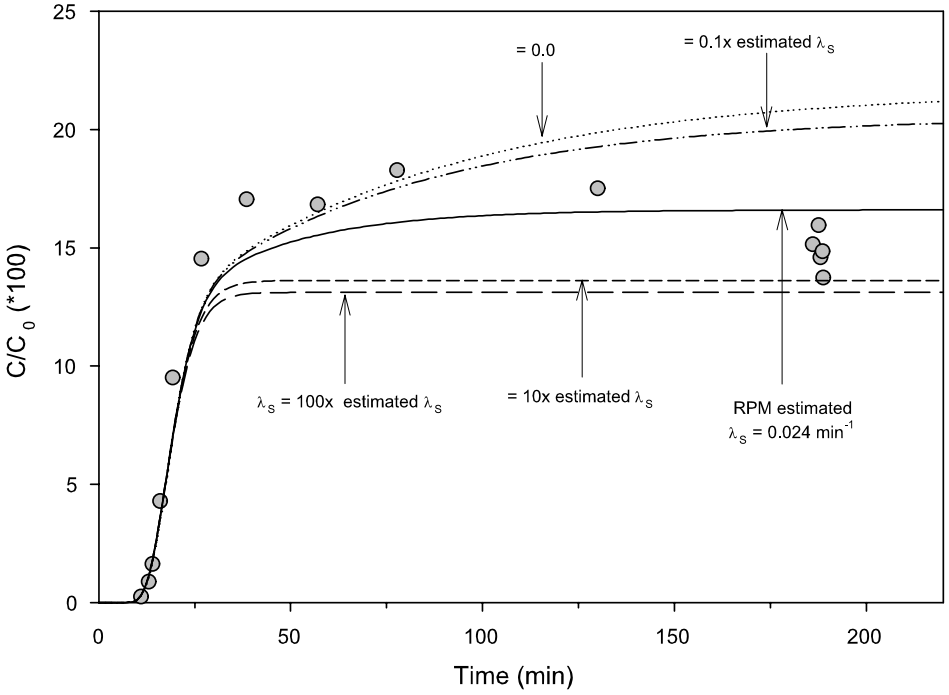

Fig. 5. The sensitivity of reactive transport model to variation in λ_S, May 2000.

return to the advective zone within the time frame of these experiments. In contrast, variation in λ_C influences the plateau concentration of NO_3–^{15}N, which was accurately predicted in this analysis.

As a means of assessing the validity of our results, we now review the relationships between several hydrological and assimilatory residence times. We begin by calculating the total amount of NO_3–^{15}N retained in our reach, then evaluate whether hydrologic and assimilatory residence times in both channel and storage environments combine to explain the magnitude of retention observed in these experiments. The fraction of added tracer retained in each experiment can be calculated using predictions of uptake length (S_W) and reach length (L) within the exponential loss model (fraction retained $= 1 - (\exp(-L/S_W))$). This calculation indicates that approximately 87% and 76% of the tracer NO_3–^{15}N was retained with the reach in the September and May experiments, respectively. If transient storage were absent from the reach on these dates, median travel times would have been 54.0 and 24.6 min in September and May, respectively ($= T_{med} * (1 - F_{med})$) [39]. Using estimates of λ_C, that period of time would have resulted in 71% and 57% removal of the NO_3–^{15}N tracer.

However, the transient storage modeling indicated that 64% and 42% of the conservative tracer entered the storage zone ($= 1 - \exp(-L/L_S)$) within the reach during September and May, respectively. Once in storage, mean hydrologic and assimilatory residence times combine to predict that 64% and 73% of the entrained NO_3–^{15}N would be removed, respectively. In the absence of uptake in the channel (advective zone), the likelihood of entry into the transient storage zone, hydrologic residence time, and λ_S combine to predict that 41% and 42% of the added NO_3–^{15}N tracer would be removed within the reach by activity in the transient storage zone alone. In each case (only channel or transient storage activity), the estimated hydrologic and assimilatory residence times combine to predict retention rates less than those observed.

The estimates derived above represent the maximum contribution each compartment could make to NO_3–^{15}N retention within the reach. Over the time scales assessed in this study, molecules assimilated in one habitat (e.g. the channel) are not available for assimilation in the other (e.g. transient storage zone). Therefore, the percentages estimated above are not additive. The RPM estimated that the transient storage zone accounted for 44% and 49% of the retention occurring in the reach. Multiplying U_S/U estimates by total percent retention in the reach (from above) predicts that 36% and 32% of the NO_3–^{15}N retention occurred in the transient storage zone. By difference, the RPM predicts that the remaining 51% and 44% was retained in the channel compartment. These percentages can be viewed as the realized percent retention within a given compartment. If the partitioning of uptake is accurate, the ratio of realized retention and maximum retention would be equal in each compartment. In fact, in May these ratios are nearly equivalent (0.76 and 0.77, respectively), but differ in September (channel = 0.71, transient storage = 0.88) suggesting that the U_S/U estimate may be

slightly high on this date. Regardless, the preceding assessment clearly indicates that the U_S/U estimates generated by the RPM closely reflect conditions in the field.

The RPM analysis indicates that the hyporheic zone of Snake Den Branch is an important sink for stream water NO_3. Further evidence in support of this conclusion comes from our calculation of the hyporheic reaction significance factor (RSF). Harvey and Fuller [19] developed the RSF to assess the importance of the hyporheic zone in retaining manganese, but to our knowledge, this metric has yet to be applied to nutrient biogeochemistry in streams. In each case, RSF estimates in this study indicated that the hyporheic zone exerted a substantial influence on stream water nitrate concentrations in Snake Den Branch. During May and September, RSF values were approximately 3 and 4 times the suggested threshold value ($RSF > 0.2$) [19]. More research will be required to assess how Snake Den Branch compares to other systems in terms of the propensity for storage zones to impact nutrient retention. Further, we anticipate that the influence of the storage zone will reflect both the hydrologic and biological features that may exist in various combinations across the diversity of stream ecosystems.

6. Summary

Relatively few studies have addressed how natural variation in rates of subsurface metabolic and biogeochemical processes influence the transport and retention of nutrients in stream ecosystems. In the preceding exercise, the method of Mulholland et al. [34] was revised to provide a more quantitative approach for estimating channel uptake. The resulting Regression Partitioning Method (RPM) is a numerical technique that relies on time series data from a downstream transect to establish a correlation between a measure of reactive tracer abundance (i.e. NO_3–N:Cl ratio) and the percentage of tracer that has resided within, and returned from, the transient storage zone (i.e. hyporheic zone). The percentage of tracer that has resided in the storage zone is obtained by manipulating the appropriate one-dimensional transport with transient storage model. Partitioning uptake between the channel and storage zone is accomplished by regressing these variables and completing a series of numerical manipulations. Applying the RPM to Snake Den Branch, a small headwater stream in western North Carolina, determined that the transient storage zone accounted for ~44–49% of total NO_3–N retention. Converting RPM results to estimates of channel and storage zone reaction rate constants (λ_C and λ_S) illustrated that the RPM produced estimates that closely resembled field data in magnitude and pattern. The rarity of data regarding the contribution of the hyporheic zone to nutrient retention in streams has largely been due to the absence of an easy and affordable technique for quantifying the phenomenon. The Regression Partitioning Method is an attempt to fill that void and its application in other streams will likely contribute to our knowledge of the role of the hyporheic zone in stream ecosystems.

References

[1] Baker MA, Dahm CN, Valett HM. Anoxia, anaerobic metabolism, and biogeochemistry of the stream-water–ground water interface. In: Jones JB, Mulholland PJ, editors. Streams and ground waters. San Diego, CA: Academic Press; 2000. p. 259–83.
[2] Baker MA, Valett HM, Dahm CN. Organic carbon supply and metabolism in a shallow groundwater ecosystem. Ecology 2000; 81:3133–48.
[3] Bencala KE. A perspective on stream-catchment connections. J North Am Benthol Soc 1993;12:44–7.
[4] Bencala KE, Walters RA. Simulation of solute transport in a mountain pool-and-riffle stream: a transient storage model. Water Resour Res 1983;19:718–24.
[5] Bencala KE, Kennedy VC, Zellweger GE, Jackman AP, Avanzino RJ. Interactions of solutes and streambed sediment 1. An experimental analysis of cation and anion transport in a mountain stream. Water Resour Res 1984;20:1797–803.
[6] Boulton AJ, Findlay S, Marmonier P, Stanley EH, Valett HM. The functional significance of the hyporheic zone in streams and rivers. Annu Rev Ecol Syst 1998;29:59–81.
[7] Bretschko G, Leichtfried M. Distribution of organic matter and fauna in a second order, alpine gravel stream Ritrodat-Lunz area, Austria. Verh Internat Verein Theor Angew Limnol 1988;23: 1333–9.
[8] Butturini A, Sabater F. Importance of transient storage zones for ammonium and phosphate retention in a sandy-bottom Mediterranean stream. Freshwater Biol 1999;41:593–603.
[9] Dahm CN, Trotter EH, Sedell JR. Role of anaerobic zones and processes in stream ecosystem productivity. In: Averett RC, McKnight DM, editors. Chemical quality of water and the hydrologic cycle. Chelsea, MI: Lewis Publishers; 1987. p. 157–78.
[10] D'Angelo DJ, Webster JR, Gregory SV, Meyer JL. Transient storage in Appalachian and Cascade mountain streams as related to hydraulic characteristics. J North Am Benthol Soc 1993;12: 223–35.
[11] Dent CL, Schade JD, Grimm NB, Fisher SG. Subsurface influences on surface biology. In: Jones JB, Mulholland PJ, editors. Streams and ground waters. San Diego, CA: Academic Press; 2000. p. 381–402.
[12] Duff JH, Triska FJ. Denitrification in sediments from the hyporheic zone adjacent to a small forested stream. Can J Fish Aquat Sci 1990;47:1140–7.
[13] Fellows CS, Valett HM, Dahm CN. Whole-stream metabolism in two montane streams: Contribution of the hyporheic zone. Limnol Oceanogr 2001;46:523–31.
[14] Findlay S. Importance of surface–subsurface exchange in stream ecosystems: The hyporheic zone. Limnol Oceanogr 1995;40: 159–64.
[15] Grimm NB, Fisher SG. Exchange between interstitial and surface water: implications for stream metabolism and nutrient cycling. Hydrobiologia 1984;111:219–28.
[16] Hall Jr RO, Bernhardt ES, Likens GE. Relating nutrient uptake with transient storage in forested mountain streams. Limnol Oceanogr 2002;47:255–65.
[17] Hart BT, Freeman P, McKelvie ID. Whole-stream phosphorus release studies: variation in uptake length with initial phosphorus concentration. Hydrobiologia 1992;235/236:573–84.

[18] Hart DR. Parameter estimation and stochastic interpretation of the transient storage model for solute transport in streams. Water Resour Res 1995;29:89–98.
[19] Harvey JW, Wagner BJ. The physical template: hydrology, hydraulics, and physical structure. In: Jones JB, Mulholland PJ, editors. Streams and ground waters. San Diego, CA: Academic Press; 2000. p. 43–4.
[20] Harvey JW, Fuller CC. Effect of enhanced manganese oxidation in the hyporheic zone on basin-scale geochemical mass balance. Water Resour Res 1998;34:623–36.
[21] Harvey JW, Wagner BJ, Bencala KE. Evaluating the reliability of the stream tracer approach to characterize stream–subsurface water exchange. Water Resour Res 1996;32:2441–51.
[22] Hatcher Jr RD. Bedrock geology and regional geologic setting of Coweeta Hydrologic Laboratory in the Eastern Blue Ridge. In: Swank WT, Crossley Jr DA, editors. Forest hydrology and ecology at Coweeta. New York, NY, USA: Springer-Verlag; 1988. p. 81–102.
[23] Hendricks SP, White DS. Physicochemical patterns within a hyporheic zone of a northern Michigan river, with comments on surface water patterns. Can J Fish Aquat Sci 1991;48:1645–54.
[24] Holmes RM, Jones JB, Fisher SG, Grimm NB. Denitrification in a nitrogen-limited stream ecosystem. Biogeochemistry 1996;33: 125–46.
[25] Johnson EA, Kovner JL. Effect on streamflow of cutting a forest understory. Forest Sci 1956;2:82–91.
[26] Jones JB, Mulholland PJ, editors. Streams and ground waters. San Diego, CA, USA: Academic Press; 2000.
[27] Jones Jr JB, Fisher SG, Grimm NB. Vertical hydrologic exchange and ecosystem metabolism in a Sonoran Desert stream. Ecology 1995;76:942–52.
[28] Kimball BA, Broshears RE, Bencala KE, McKnight DM. Coupling of hydrologic transport and chemical reactions in a stream affected by acid mine drainage. Environ Sci Technol 1994;28:2065–73.
[29] Marti E, Grimm NB, Fisher SG. Pre- and post-flood retention efficiency of nitrogen in a Sonoran Desert stream. J North Am Benthol Soc 1997;16:805–19.
[30] Metzler GM, Smock LA. Storage and dynamics of subsurface detritus in a sand-bottomed stream. Can J Fish Aquat Sci 1989;47:588–94.
[31] Morrice JA, Dahm CN, Valett HM, Unnikrishna PV, Campana ME. Terminal electron accepting processes in the alluvial sediments of a headwater stream. J North Am Benthol Soc 2000;19:593–608.
[32] Mulholland PJ, DeAngelis DL. Surface–subsurface exchange and nutrient spiraling. In: Jones JB, Mulholland PJ, editors. Streams and ground waters. San Diego, CA: Academic Press; 2000. p. 149–66.
[33] Mulholland PJ, Tank JL, Sanzone DM, Wollheim WM, Peterson BJ, et al. Nitrogen cycling in a forest stream determined by a N15 tracer addition. Ecol Monogr 2000;70:471–93.
[34] Mulholland PJ, Marzolf ER, Webster JR, Hart DR, Hendricks SP. Evidence that hyporheic zones increase heterotrophic metabolism and phosphorus uptake in forest streams. Limnol Oceanogr 1997;42:443–51.
[35] Mulholland PJ, Steinman AD, Marzolf ER, Hart DR, DeAngelis DL. Effect of periphyton biomass on hydraulic characteristics and nutrient cycling in streams. Oecologia 1994;98:40–7.
[36] Mulholland PJ, Steinman AD, Elwood JW. Measurement of phosphorus uptake length in streams: comparison of Radiotracer and stable PO4 releases. CanJ Fish Aquat Sci 1990;47:2351–7.
[37] Newbold JD, Elwood JW, O'Neill RV, Van Winkle W. Measuring nutrient spiralling in streams. Can J Fish Aquat Sci 1981;38: 860–3.
[38] Peterson BJ, Wolheim WM, Mulholland PJ, Webster JR, Meyer JL, et al. Control of nitrogen export from watersheds by headwater streams. Science 2001;292:86–90.
[39] Runkel RL. A new metric of describing transient storage in streams. J North Am Benthol Soc 2002;21:529–43.
[40] Runkel RL. Using OTIS to model solute transport in streams and rivers. USGS Water Resources Fact Sheet FS-138-99, 2000.
[41] Runkel RL. One-dimensional transport with inflow and storage (OTIS): A solute transport model for streams and rivers. US geological Survey Water-Resources Investigation report 98-4018. US Geologica, Survey, Denver, CO, 1998. Available from: <http://co.water.usgs.gov/otis>.
[42] Sigman DM, Altabet MA, Michener R, McCorkle DC, Fry B, Holmes RM. Natural abundance-level measurement of nitrogen isotopic composition of oceanic nitrate: and adaptation of the ammonium diffusion method. Mar Chem 1997;57:227–42.
[43] Tank JL, Meyer JL, Sanzone DM, Mulholland PJ, Webster JR, Peterson BJ, et al. Analysis of nitrogen cycling in a forest stream during autumn using a N-tracer addition. Limnol Oceanogr 2000;45:1013–29.
[44] Thackston EL, Schnelle KB. Predicting the effects of dead zones on stream mixing. J Sanit Eng Div, ASCE 1970;96:319–31.
[45] Thomas SA, Newbold JD, Monaghan MT, Minshall GW, Georgian T. The influence of particle size on seston deposition in streams. Limnol Oceanogr 2001;46:1415–24.
[46] Thomas SA, Valett HM, Mulholland PJ, Fellows CS, Webster JR, Dahm CN, et al. Nitrogen retention in headwater streams: The influence of groundwater–surface water exchange. Sci World 2001;1:623–31.
[47] Triska FJ, Duff JH, Avanzino RJ. Influence of exchange between the channel and hyporheic zone on $NO3^-$ production in a small mountain stream. Can J Fish Aquat Sci 1990;11:2099–111.
[48] Triska FJ, Kennedy VC, Avanzino RJ, Zellweger GW, Bencala KE. Retention and transport of nutrients in a third-order stream in northwestern California: Hyporheic processes. Ecology 1989;70:1893–905.
[49] Valett HM, Dahm CN, Campana ME, Morrice JA, Baker MA, et al. Hydrologic influences on groundwater–surface water ecotones: heterogeneity in nutrient composition and retention. J North Am Benthol Soc 1997;16:239–47.
[50] Valett HM, Morrice JA, Dahm CN, Campana ME. Parent lithology, groundwater–surface water exchange and nitrate retention in headwater streams. Limnol Oceanogr 1996;41:333–45.
[51] Valett HM, Fisher SG, Grimm NB, Camill P. Vertical hydrologic exchange and ecological stability of a desert stream ecosystem. Ecology 1994;75:548–60.
[52] Valett HM, Fisher SG, Stanley EH. Physical and chemical characteristics of the hyporheic zone of a Sonoran desert stream. J North Am Benthol Soc 1990;9:201–15.
[53] White DS. Perspectives on defining and delineating hyporheic zones. J North Am Benthol Soc 1993;12:61–9.
[54] Wroblicky GJ, Campana ME, Valett HM, Dahm CN. Seasonal variation in surface–subsurface water exchange and lateral hyporheic area of two stream-aquifer systems. Water Resour Res 1998;34:317–28.